

Propagation of errors from a null balance terahertz reflectometer to a sample's relative water content

This article has been downloaded from IOPscience. Please scroll down to see the full text article.

2009 J. Phys.: Conf. Ser. 178 012012

(<http://iopscience.iop.org/1742-6596/178/1/012012>)

View [the table of contents for this issue](#), or go to the [journal homepage](#) for more

Download details:

IP Address: 134.225.69.51

The article was downloaded on 22/03/2013 at 12:40

Please note that [terms and conditions apply](#).

Propagation of errors from a null balance terahertz reflectometer to a sample's relative water content

S. Hadjiloucas¹, G.C. Walker¹, J. W. Bowen¹ and A. Zafirooulos²

¹Cybernetics, School of Systems Engineering, The University of Reading, RG6 6AY, UK

²Biosystems Engineering Department, School of Agricultural Technology, Technological Educational Institute of Larissa, 411 10, Larissa, Greece.

email: s.hadjiloucas@reading.ac.uk

Abstract. The THz water content index of a sample is defined and advantages in using such metric in estimating a sample's relative water content are discussed. The errors from reflectance measurements performed at two different THz frequencies using a quasi-optical null-balance reflectometer are propagated to the errors in estimating the sample water content index.

1. Performing absolute reflectance measurements at THz frequencies

Quasi-optical null-balance polarimetric bridge techniques [1, 2] may be used to measure the complex reflectance or transmittance of planar structures at any frequency between 100 GHz and 2.5 THz. In the system depicted in Figure 1, the beam from the source is transmitted through a vertically oriented wire grid to ensure polarisation purity and is split equally into two orthogonal polarisation components using a 45° grid. Each component of the beam takes a different path through the instrument: one beam (the sample beam), is normally incident on the sample, whilst the second, the reference beam, is normally incident on the reference grid. The two reflected beams are recombined using an appropriately oriented 45° wire grid polarising beam-splitter. The interferometer is balanced in phase using a translation stage when the two path lengths are equal. When the instrument is also balanced in amplitude, by rotating the grid in the reference arm so that its reflectance matches that of the sample, a null voltage is observed at the detector. Two measurements are performed, one with the sample in place and another using a polished flat metallic surface (which is assumed to be a perfect THz reflector) replacing the sample. In both cases the instrument is balanced in amplitude and phase by rotating the grid and changing the path length in the reference arm.

In well aligned instruments built using a quasi optical breadboard, half-cubes, and high density polyethylene lenses separated by 3 half cube distances, as the one shown in Figure 1 marketed by Thomas Keating Ltd., the typical fringe visibility is of the order of 10^5 . This figure assumes the use of an amplitude modulated Gunn source (Photonics Innovation Centre, St Andrews) with a power output around 10 mW operating at 100 GHz. The signal is detected using a Flann microwave crystal detector and demodulated using a lock-in amplifier.

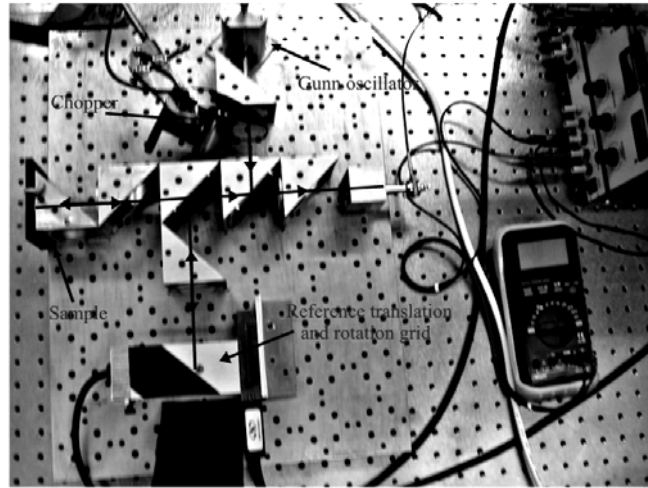


Figure 1. Top view of a quasi-optical null-balance reflectometer made of HDPE lenses and grids mounted on half cubes.

Using Jones matrix analysis to describe the electric field in the reference and sample arms of the interferometer [1, 2] when this is balanced in both amplitude and phase, one can calculate the THz reflectivity of the sample R from an angle γ , which corresponds to the half angle between adjacent nulls recorded sequentially with the sample and reference reflector in place:

$$R = \sin^2 \gamma \quad (1)$$

The measured sample reflectance is referenced to the impedance of free space and is therefore an absolute measurement.

2. Linking a sample's THz reflectance to its relative water content

The analysis of canopy temperature and vegetation indices using infrared and near infrared reflectance from satellite radiometry has prompted scientists to develop signal processing routines that would enable them to extract additional information such as plant relative water content (RWC) in the hope that the degree of water stress and the onset of drought can be predicted. Previous work concentrated on the analysis of ratios formed between these two bands. In a seminal paper, Hunt *et al.*, [3] proposed a new leaf water content index (WCI) which would directly correlate sample reflectance to relative water content; this index was subsequently used extensively by plant physiologists to remotely assess the onset of water stress across large agricultural areas and the impact of pollution in the environment. Their argument was that the difference between reflectance at a particular infrared frequency band for a dry sample to that of a fresh sample should be equal to the absorbance by water in that sample. By normalising this difference in reflectance to that obtained at another frequency band where the reflectance was insensitive to a change in water content, it is possible to normalise the values to account for the water content present. Their work led to the derivation of a very ingenious water content index defined as follows:

$$WCI = \frac{-\ln[1 - (R_{\Delta f 1}^{in-situ} - R_{\Delta f 2}^{in-situ})]}{-\ln[1 - (R_{\Delta f 1}^{full-turgor} - R_{\Delta f 2}^{full-turgor})]} \quad (2)$$

where subscripts to the reflectance $\Delta f1$ and $\Delta f2$ correspond to the spectral bands and superscripts refer to an *in-situ* and at *full-turgor* reflectance from the sample surface during the calibration measurement process. This index was found [3] to be directly related to relative water content (1:1 correspondence).

Simulations of *WCI* values assuming all possible values for the difference between $R_{\Delta f1}^{in-situ}$ and $R_{\Delta f2}^{in-situ}$ (1-99%) assuming different values (a-e) for the difference $R_{\Delta f1}^{full-turgor} - R_{\Delta f2}^{full-turgor}$ are shown in Figure 2 below.

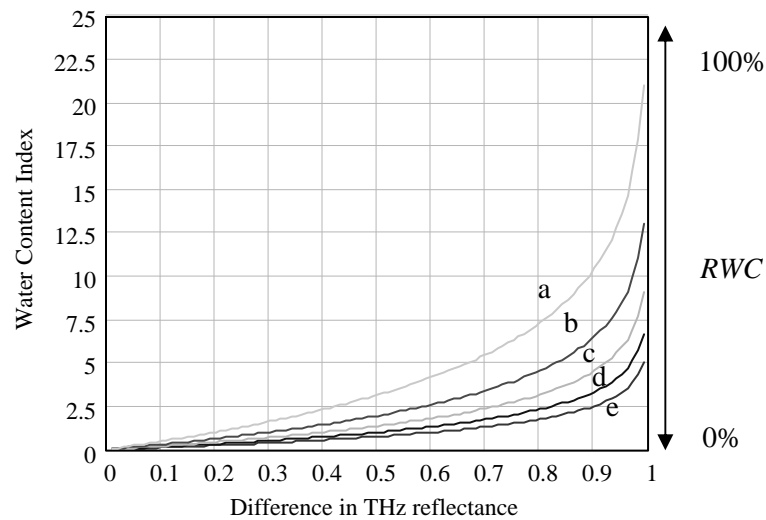


Figure 2. Variation of the THz water content index (*WCI*) as a function of the in-situ reflectance - numerator in expression in (2) for different values of the denominator corresponding to full turgor reflectance difference set to a) 0.2, b) 0.3 c) 0.4, d) 0.5 e) 0.6. The corresponding span of relative water content values (*RWC*) is also shown.

Two conclusions can be drawn from Figure 2. Firstly a THz passive radiometric system would be superior in extracting relative water content information to an infrared system because absorption lines at THz frequencies relative to those at the infrared are stronger (as long as the signal is not completely attenuated due to atmospheric absorption). Secondly, the precision in determining the water content index improves (a higher slope in Figure 2) when choosing one channel at a line strongly absorbing at THz frequencies and another channel at a weak line.

Adopting this technique for the THz part of the spectrum to analyse measurements of a sample's water content using the null balance reflectometer is sound. Such an approach would require the quasi-optical system to be appropriately modified to perform the measurements at two spectral bands simultaneously. Although in principle, with the use of additional quasi-optical components and diplexers this should be possible, in practice, for samples where their water content does not change rapidly, the current system is adequate to perform the measurements sequentially by re-tuning the source to two spectral bands. A small change in the magnitude of standing waves at the two frequency bands due to multiple reflections at the lens interfaces would have to be tolerated under such a mode of operation because the optical properties of high density polyethylene (HDPE) can change significantly above 300 GHz. Using newer proprietary polymer materials to make the lenses (e.g., TSURUPICA marketed by Microtech Instruments), should minimize this problem in high frequency implementations. In addition, the overall effect in the measured reflectance should also be minimal because an equal number of lenses is present in both the measurement and sample arms of the interferometer (balanced realization).

By analogy to the work reported in [3], the proposed index for the THz part of the spectrum is:

$$WCI_{THz} = \frac{-\ln[1 - (\sin^2(\gamma)_{\Delta fTHz1}^{in-situ} - \sin^2(\gamma)_{\Delta fTHz2}^{in-situ})]}{-\ln[1 - (\sin^2(\gamma)_{\Delta fTHz1}^{full-turgor} - \sin^2(\gamma)_{\Delta fTHz2}^{full-turgor})]} \quad (3)$$

with superscripts and subscripts retaining their usual meaning. This expression is useful as it can translate the measured ambiguity in the water content index to the performance characteristics of the reflectometer under different realizations.

The requirement to perform 8 measurements (four with the sample as shown in (3) and four with the reference reflector to account for differences in reflectance at the two channel frequencies), introduces additional errors in the determination of the sample's water content index. It is possible to predict the uncertainty in WCI_{THz} for an uncertainty in the reflectance terms due to the inability of the user (under manual operation) or the limitations in hardware or software (automated operation) in resolving the most balanced state possible for the reflectometer using an error propagation analysis. Assuming that the precision in measuring the reflectivity of a metal reflector $\delta R_i^{reflector}$, where $i=1..4$ remains the same over the four required measurements, for the four additional measured quantities required to de-embed the water content index, we generate a vector of measurements $(x_1 \ x_2 \ x_3 \ x_4 \ R_1^{reflector} \ R_2^{reflector} \ R_3^{reflector} \ R_4^{reflector})$ and assume that:

$$WCI_{THz} = f(x_1 \ x_2 \ x_3 \ x_4 \ R_1^{reflector} \ R_2^{reflector} \ R_3^{reflector} \ R_4^{reflector}) \quad (4a)$$

where:

$$\begin{aligned} x_1 &= \sin^2 \gamma_a \equiv \sin^2(\gamma)_{\Delta fTHz1}^{in-situ} \\ x_2 &= \sin^2 \gamma_b \equiv \sin^2(\gamma)_{\Delta fTHz2}^{in-situ} \\ x_3 &= \sin^2 \gamma_c \equiv \sin^2(\gamma)_{\Delta fTHz1}^{full-turgor} \\ x_4 &= \sin^2 \gamma_d \equiv \sin^2(\gamma)_{\Delta fTHz2}^{full-turgor} \end{aligned} \quad (4b)$$

The total uncertainty in WCI_{THz} from the 8 measurements is given from:

$$\delta WCI_{THz} = \sqrt{\sum_{i=1}^4 \left(\frac{\partial WCI_{THz}}{\partial x_i} \delta x_i \right)^2 + 4 \left(\delta R^{reflector} \right)^2} \quad (5)$$

where δx_i is the error in each measurement with the sample in place. Observing that $1 - \sin^2 \gamma_i = \cos^2 \gamma_i$ and $2 \sin \gamma_i \cos \gamma_i = \sin 2\gamma_i$, the relevant partial derivatives are:

$$\frac{\partial(WCI_{THz})}{\partial \gamma_a} = -\frac{\sin 2\gamma_a}{(\sin^2 \gamma_b + \cos^2 \gamma_a) \ln(\sin^2 \gamma_d + \cos^2 \gamma_c)} \quad (6a)$$

$$\frac{\partial(WCI_{THz})}{\partial \gamma_b} = \frac{\sin 2\gamma_b}{(\sin^2 \gamma_b + \cos^2 \gamma_a) \ln(\sin^2 \gamma_d + \cos^2 \gamma_c)} \quad (6b)$$

$$\frac{\partial(WCI_{THz})}{\partial \gamma_c} = \frac{\sin 2\gamma_c \ln(\sin^2 \gamma_b + \cos^2 \gamma_a)}{(\sin^2 \gamma_d + \cos^2 \gamma_c) \ln(\sin^2 \gamma_d + \cos^2 \gamma_c)^2} \quad (6c)$$

$$\frac{\partial(WCI_{THz})}{\partial\gamma_d} = -\frac{\sin 2\gamma_d \ln(\sin^2 \gamma_b + \cos^2 \gamma_a)}{(\sin^2 \gamma_d + \cos^2 \gamma_c) \ln(\sin^2 \gamma_d + \cos^2 \gamma_c)^2} \quad (6d)$$

The justification for assuming different values for the error in each of the reflectance terms can be found in previous work [2]. As also described in [2], one can further propagate these errors to more fundamental quantities related to the operation of the reflectometer such as the error in determining the rotating grid angle $\sigma_{\gamma_{TOTAL}}$ and an error in determining the translation position in the roof-top reflector $\sigma_{d_{TOTAL}}$, after specifying a source output power P_o , a noise equivalent power NEP at the detector, as well as a post-detection bandwidth B for the lock-in amplifier.

3. Discussion

For the technique to be useful, measurements with a sample at full turgor, where water content is maximum, are necessary. Furthermore, because the reflectometer must always be balanced in phase in order to provide an accurate measurement of reflectance, the sample should present a well defined flat surface across the beam. At THz frequencies, to a certain extent, some surface irregularity can be tolerated because at 1 THz the wavelength is 300 μm . Pseudo-coherence error (loss of interferometric modulation due to variability of the sample's thickness across the beam) compensation might have to be considered if the sample's surface is grooved or patterned in a defined way.

Although the contour plot that relates normalised power output as a function of reflector down-beam distance and grid angle is supposed to be symmetric, in practice, the multiple nulls observed across the landscape do not show the same fringe visibility. This is due to a beam dilution effect when the lengths of the sample and reference arms of the reflectometer are not exactly the same. For brevity, in this work, errors in the measured reflectivity due to such beam dilution effects are not propagated analytically to the water content index. Such errors are more pronounced at lower frequencies where the diffractive spreading of the beam between adjacent half cubes is more pronounced.

4. Conclusion

A quasi-optical null-balance bridge reflectometer is used to measure the complex reflectance of samples at THz frequencies. A novel de-embedding procedure for estimating the water content in biological tissue is proposed and its precision is analytically derived taking into consideration measurement errors from a sequence of measurements. The analysis provides estimates of the water content index of a sample so that its relative water content can be inferred.

References

- [1] S. Hadjiloucas, L.S. Karatzas and J.W. Bowen (1999). 'Measurements of Leaf Water Content Using Terahertz Radiation,' *IEEE Transactions on Microwave Theory and Techniques MTT*, **47**, 142-149.
- [2] S. Hadjiloucas and J.W. Bowen (1999). 'The Precision of Quasi-optical Null-Balanced Bridge Techniques for Transmission and Reflection Coefficient Measurements,' *Review of Scientific Instruments*, **70**, 213-219.
- [3] E. R. Hunt Jr., B. N. Rock and P.S. Nobel (1987), 'Measurement of leaf relative water content by infrared reflectance,' *Remote Sensing of Environment*, **22**, 429-435.